Activity and Diversity of Methanotrophic Bacteria at Methane Seeps in Eastern Lake Constance Sediments[▽]

Jörg S. Deutzmann, Susanne Wörner, and Bernhard Schink*

Fachbereich Biologie, Universität Konstanz, D-78457 Constance, Germany

The activity and community structure of aerobic methanotrophic communities were investigated at methane seeps (pockmarks) in the littoral and profundal zones of an oligotrophic freshwater lake (Lake Constance, Germany). Measurements of potential methane oxidation rates showed that sediments inside littoral pockmarks are hot spots of methane oxidation. Potential methane oxidation rates at littoral pockmark sites exceeded the rates of the surrounding sediment by 2 orders of magnitude. Terminal restriction fragment length polymorphism (T-RFLP) analysis of the *pmoA* gene revealed major differences in the methanotrophic community composition between littoral pockmarks and the surrounding sediments. Clone library analysis confirmed that one distinct *Methylobacter*-related group dominates the community at littoral pockmarks. In profundal sediments, the differences between pockmarks and surrounding sediments were found to be less pronounced.

Methane is an effective greenhouse gas and accounts for 18% of the radiative forcing caused by long-lived greenhouse gases (27). The relative contribution of different sources to the global atmospheric methane pool is being discussed (8, 41), and the importance of freshwater lakes is especially a matter of dispute (3, 13, 16). Aerobic methane-oxidizing bacteria (MOB) play an important role in mitigating methane emission from freshwater environments, as they oxidize methane to carbon dioxide in the presence of oxygen (42). In Lake Constance, Germany, MOB oxidize aerobically more than 90% of the methane formed in deeper sediment layers by methanogenic archaea (17).

In undisturbed sediments, stable gradients of methane and oxygen are formed (42). MOB shape these gradients by consuming methane and oxygen in a way that the two substrates meet only in a narrow zone due to limited diffusive transport (34, 39). With the establishment of such a gradient system, the bacterial community constantly experiences very low substrate concentrations, which select within the community for strains with higher substrate affinities (34).

Pockmarks are concave depressions of the sediment surface which have so far been observed mainly in marine sediments (24, 25, 28). Reports of pockmarks in freshwater habitats are still rare (14, 36). In the last years, hundreds of pockmark-like structures were discovered in the southeastern part of Lake Constance (50). These pockmarks are round depressions of up to 8 m diameter and 0.5 to 1.5 m depth. At 40% of these sites, biogenic methane was observed to bubble out of the sediment (6). In shallow areas of the lake that exhibit enhanced productivity, these gas bubbles can reach the water surface and emit methane to the atmosphere (50).

Environmental conditions in sediments close to the gas-emitting sites are likely to differ drastically from the conditions in undisturbed sediment. Close to the gas emanation sites, both oxygen and methane are probably available in excess. Methane from gas bubbles can dissolve into the well-oxygenated water and diffuse into the sediments, leading to high local methane concentrations and potentially high diffusive methane fluxes. Additionally, water movements might be caused by the upwelling bubbles, which may increase convective mixing of both methane and oxygen. Therefore, methanotrophic bacteria situated at those sites likely encounter higher substrate concentrations there than in the surrounding sediment.

The community composition, diversity, abundance, and distribution of MOB in the well-stratified and undisturbed profundal sediments as well as in the wind- and wave-exposed littoral sediments of Lake Constance have been investigated (35, 39, 40). In the present study, we investigated the MOB community composition at pockmark sites and compared it to the compositions of the communities in the surrounding sediment outside the pockmarks. In addition, the methane oxidation potential of the communities was measured to examine whether the escaping methane increases the methane oxidation activity of MOB communities at these sites.

MATERIALS AND METHODS

Sampling. Pockmarks that were previously located and mapped (50) were relocated by use of the Global Positioning System (GPS), and a horizontally scanning sonar was employed for exact positioning of the sediment corers. At the first cruise on 26 April 2010, profundal pockmark samples (PP) were taken with a gravity multicorer with plastic tubes of 60 mm inner diameter in the southeastern part of Lake Constance (47°31.37755N, 9°35.89464E) at 82 m water depth. Profundal reference sediment outside the pockmark (PR) was taken approximately 50 m away (47°31.37151336N, 9°35.91289522E), also at 82 m water depth. The littoral pockmark (LP1) was sampled at 12 m water depth by scuba diving with plastic tubes of 80 mm inner diameter to sample the gas ebullition site reliably (47°29.97485222N, 9°35.70826669E), whereas littoral reference sediment outside the pockmark (LR1) was collected at 12 m water depth with the same corer used for profundal samples (47°29.95212802N, 9°36.13246003E).

At a second cruise on 15 June 2010, only littoral samples were taken by scuba diving. Two gas ebullition sites in pockmarks (LP2, LP3) were sampled with

---

plastic tubes of 80 mm inner diameter (LP2, 47°29.97538772N, 9°35.7090691E, and LP3, 47°29.97593976N, E 9°35.7066863E). Reference sediment cores (LR2 and LR3) were taken by divers outside the respective pockmark with two 50-ml Falcon tubes with a small hole in the bottom to release the overlying water during sampling. Samples taken with the multicorer were cut directly on board and then cooled. Samples taken by divers were transported as undisturbed sediment core to the lab. All samples were cooled during transport to the laboratory.

Methane oxidation capacities. Samples for determination of methane oxidation capacities were stored overnight at 4°C and processed on the next day. Sediment material from the uppermost 4 cm of each core was suspended 1:2 (wt/wt) with sterile freshwater medium (7) and mixed well under nitrogen gas to prevent oxidative stress during methane starvation. Twenty milliliters slurry was prepared in 58-ml serum bottles under a headspace of 25% air ($\sim$5% O_2) and 75% nitrogen. Samples LR2 and LR3 were treated similarly, but 10 ml slurry was incubated in 23-ml serum bottles. Methane was added to the headspace to provide final concentrations of 0.05, 0.1, 0.2, 0.4, 0.7, 1.0, and 2.0% (vol/vol) and, for incubation of sample LP1, also 4.0%. Vials were incubated at the *in situ* temperature (4°C for 1st cruise, 13°C for 2nd cruise) in a horizontal linear shaker. Initial methane oxidation rates were calculated from the determined methane concentration decrease over time. The rates for LP and profundal samples were measured over 5 to 8 h on the first day. On the second day, the gas phase was renewed and methane decrease was monitored again over 8 h. Maximum methane oxidation capacities (V_{max}s) and apparent half-saturation constants ($S_{0.5}$s) were calculated with second-day data sets because the sampling intervals chosen on the first day were too long to get trustworthy results from some pockmark slurries (methane was consumed almost completely at low concentrations at the second data acquisition point). The methane decrease in LR samples was monitored for up to 5 days. Methane was determined with a 6000 Vega series 2 gas chromatograph (Carlo Erba Instruments) as described previously (37). To estimate the $S_{0.5}$s and V_{max}s of the different sediment incubations, initial methane oxidation rates were plotted against the initial methane concentration, and curves were fitted using Origin software, version 6.0 (Microcal Software). Methane oxidation rates that were too low to be detected at high methane concentrations due to the high relative measurement errors were not analyzed any further. Oxygen measurements in a subset of samples during the sampling period never revealed complete oxygen depletion (<0.2% in the gas phase).

DNA extraction, T-RFLP, and clone library. DNA was extracted in duplicate from undiluted sediment slurries of the uppermost 4 cm of each sediment core immediately after arrival at the lab (2 to 5 h after sampling). A NucleoSpin soil kit (Macherey-Nagel) was used according to the manufacturer's instructions, and the products of duplicate extractions were pooled. Partial *pmoA* genes were amplified using the *pmoA* primer pair A189-mb661 (10) to cover the maximum MOB diversity without amplification of *amoA* genes (5). Terminal restriction fragment length polymorphism (T-RFLP) analysis was performed using two fluorescent primers (mb661 labeled with 6-carboxyfluorescein [mb661-FAM], A189 labeled with hexachloro-6-carboxyfluorescein [A189-HEX]) to increase the resolution of the T-RFLP analysis. PCR products were purified using a DNA Clean & Concentrator-5 kit (Zymo Research).

For T-RFLP analysis, 200 ng DNA (or 17 μl PCR mixture for negative controls) was digested with 0.5 U of the restriction enzyme MspI (Fermentas) for 3 h at 37°C according to the manufacturer's instructions. After heat inactivation at 80°C for 20 min, all samples were stored at −20°C till analysis. Terminal restriction fragments (T-RFs) were size separated in triplicate on an ABI Prism 3130xl genetic analyzer (Applied Biosystems) using an internal size standard (0.5 μl diluted in 10 μl water; GeneScan 500 ROX; Applied Biosystems) and 10 μl of digested DNA. Samples were denatured at 94°C for 5 min, immediately cooled on ice, and shortly centrifuged. T-RF sizes between 50 and 500 bp with peak heights of at least 30 fluorescence units were analyzed using GeneMapper software (version 4.0; Applied Biosystems). T-RFs present in no-template controls or in only one replicate were excluded from analysis. Despite the localization of the MspI restriction site at the very end of the mb661-FAM primer, good T-RFLP profiles were also obtained in that direction. Thus, MspI obviously cannot cut off the fluorophore at this site. T-RFLP analysis, including the additive main effects and multiplicative interaction model (AMMI), and interaction principal component analysis (IPCA) were performed using the T-REX program (version 1, revision 11; http://trex.biohpc.org/) (11). Peak height was chosen as the parameter, and data were aligned using a 1.7-bp threshold. No noise filtering was used because the filtering algorithm is not suitable for samples with a low number of T-RFs. The data set was analyzed first using T-RFLP profiles from all sites as individual samples (environments). To check for the amount of variation that can be explained by the site characteristic pockmark in the littoral zone alone, a second analysis was performed using the three littoral pockmark sites and references as replicates for littoral pockmark and reference sites, respectively.

pmoA clone libraries were constructed using a TA cloning kit (Invitrogen), and the plasmid inserts of randomly picked clones were amplified using the M13 primer pair. Subsamples of the amplified products were digested with MspI (5 U; MBI Fermentas), separated by gel electrophoresis on a 2.5 to 4% agarose gel, and grouped according to their restriction patterns. Clones from each group were randomly selected for sequencing. Undigested PCR products were digested with another restriction enzyme (TasI; Fermentas) and analyzed as mentioned above. Sequencing was carried out by GATC-Biotech Co., Constance, Germany. The quality of the sequences was checked manually. Alignment and phylogenetic analysis were done using MEGA (version 4) software (48) and the online-based software at www.phylogeny.fr. The tree shown was constructed using the minimum-evolution method in MEGA (version 4) software, selecting the pairwise deletion option (1,000 replications). Evolutionary distances were computed using the JTT matrix-based method. Clones were grouped according to their position in the phylogenetic tree.

qPCR. Quantitative real-time PCR (qPCR) was performed using 10 ng template DNA, SsoFast EvaGreen Supermix with Low ROX (Bio-Rad), and 50 nM each primer mb661 and A189 on an ABI 7500 fast machine. A primer concentration of 50 nM was chosen because higher concentrations caused an additional unspecific PCR product in some samples. A two-step PCR protocol was used, with an initial denaturation at 98°C for 2 min, followed by 40 cycles of 98°C for 6 s and 30 s at 60°C for annealing, elongation, and data acquisition. Melting curves were obtained at 60 to 95°C at a 0.5% heating rate. A plasmid (PCR2.1; Invitrogen) containing a single copy of the *pmoA* gene (GenBank accession number HQ383803) was diluted 1:10 to 10^1 to 10^7 molecules per PCR mixture and used as the standard in triplicate. Samples were analyzed in four parallel assays. PCR products were visualized via gel electrophoresis and ethidium bromide staining to exclude formation of unspecific PCR products. Analysis was done with the LinRegPCR program (43), setting individual amplification efficiencies for the different samples but using one common threshold. Cell numbers were calculated using the obtained *pmoA* copy numbers and the amount of DNA extracted from 500 mg sediment (wet weight). Two copies of the *pmoA* gene were assumed to be present per cell (29).

Nucleotide sequence accession numbers. Nucleotide sequences were deposited at the National Center for Biotechnology Information under accession numbers HQ383711 to HQ383812.

RESULTS

Sampling. Undisturbed sediment cores were obtained with all sampling methods. Since the profundal sediments had to be sampled with a multicorer, it was not possible to sample a gas emanation site exactly inside the profundal pockmark. Littoral sediment cores LP1 and LP3 showed disturbances in the sediment layers, most probably due to direct sampling of the gas emanation site. Also, some cavities were observed in deeper layers of those sediment cores during sample preparation. Core LP2 did not exhibit any indications of disturbance and is therefore likely to have been taken in the near proximity but not directly from the gas emanation site.

Methane oxidation capacities. To estimate the capacity for methane oxidation at pockmark sites, methane oxidation rates were measured at *in situ* temperature over the few days after sampling with slightly diluted sediment slurries. On average, there was an increase in methane oxidation rates on the second day to 179% of the activity on the first day in littoral samples, regardless of the initial methane concentration but with high variations between the corresponding vials of both days (standard deviation, ±104%). Profundal samples, however, showed a decrease in methane oxidation capacities between the first and the second days to a mean of 77% ± 52%, regardless of the initial methane concentration. Therefore, calculated V_{max}s have to be interpreted with caution. In addition, methane oxidation rates of LP samples (LP1, LP3) still increased with methane concentration even at high methane partial pressures
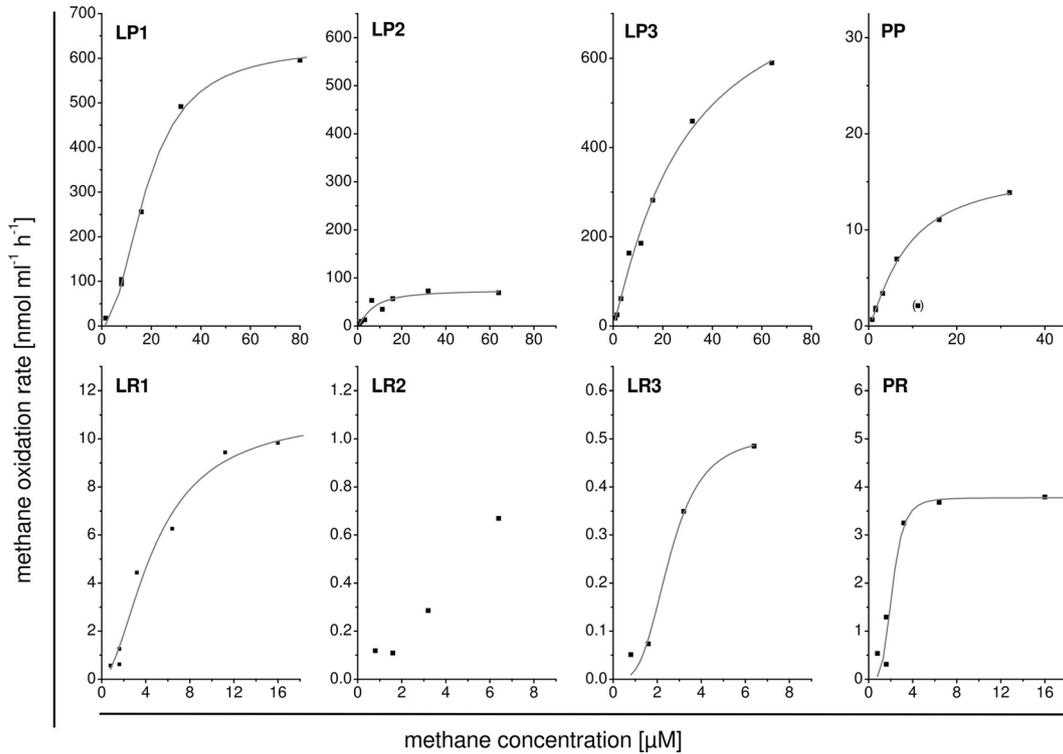
FIG. 1. Rates of methane oxidation by different sediment slurries plotted against dissolved methane concentration. Squares, measured values; lines, curve fits using the Hill equation to estimate the V_{max}s and $S_{0.5}$s of the sediment slurries.

to an extent that no definitive saturation of the methane oxidation rates was observed in those samples. This leads to error-prone estimates of V_{max} because the fitted curves have to be extrapolated (Fig. 1). Nonetheless, the calculated rates can serve as a measure for comparison between the different sites. The reference cores R2 and R3 showed only marginal methane oxidation capacities below 1 nmol ml^{-1} h^{-1}, which was below the detection limit at higher methane concentrations. In littoral pockmark slurries LP1 and LP2, V_{max}s were 627 nmol ml^{-1} h^{-1} and 831 μmol ml^{-1} h^{-1}, respectively (Table 1). Compared to the values for the reference sites outside the pockmarks, those values are higher by approximately 2 orders of magnitude (Table 1). In LP2 and the profundal cores (PP, PR), the differences were less pronounced and within 1 order of mag-

nitude (a factor of 4.3 in profundal slurries). Calculated $S_{0.5}$s for methane were higher by a factor of 3 to 6 in pockmark sediment slurries from LP1 and LP3 than in the reference sediments (Table 1).

T-RFLP analysis. Methanotrophic communities of all eight samples were compared using T-RFLP as a fast and easy fingerprint method. T-RFs with the forward primer A189-HEX (abbreviations consist of the prefix f and the T-RF size, in bp) were more diverse than T-RFs originating from the FAM-labeled reverse primer (prefix r), especially in the low-intensity T-RFs. While in samples from LR the T-RF f76 was dominant (59% ± 6%), T-RFs of the uncut PCR product (f513) showed the highest relative fluorescence intensities in profundal and LP samples (58% ± 2% and 75% ± 18%, respectively). T-RF

TABLE 1. Results of nonlinear curve fits of methane oxidation rates using the Hill equation[a] and cell numbers determined by qPCR

Sample	Chi-square	R^2	V_{max}[b]	$S_{0.5}$ (nM)	n	MOB abundance[c]
LP1	224	0.998	627 ± 21.7	18.3 ± 1.06	2.10 ± 0.17	$(2.50 ± 1.59) \times 10^9$
LP2	121	0.89	75.0 ± 14.6	6.76 ± 3.11	1.33 ± 0.61	$(2.74 ± 0.73) \times 10^7$
LP3	468	0.992	831 ± 138	28.4 ± 9.66	1.13 ± 0.17	$(1.06 ± 0.72) \times 10^9$
LR1	0.459	0.981	11.1 ± 1.46	4.81 ± 1.10	1.80 ± 0.42	$(3.72 ± 1.85) \times 10^7$
LR2	NA[d]	NA	<0.001	NA	NA	$(1.53 ± 0.53) \times 10^7$
LR3	0.002	0.986	0.51 ± 0.06	2.57 ± 0.36	3.40 ± 1.19	$(3.16 ± 0.77) \times 10^6$
PR	0.239	0.944	3.77 ± 0.37	2.15 ± 0.32	4.24 ± 1.81	$(1.02 ± 3.30) \times 10^8$
PP	0.055	0.998	16.4 ± 0.74	8.56 ± 0.85	1.28 ± 0.08	$(7.27 ± 2.12) \times 10^7$

[a] The Hill equation is $y = V_{max} \cdot x^n \cdot (x^n + k^n)^{-1}$, where y is the methane oxidation rate, x is the methane concentration, k is the half saturation constant (i.e., $S_{0.5}$), and n is the Hill coefficient.
[b] In nmol ml$_{sed}$$^{-1}$ h^{-1}.
[c] Per gram sediment (wet weight).
[d] NA, not available.

TABLE 2. Relative fluorescence signals of T-RFs with fluorescence of forward primer A189-FAM for samples from different sampling locations

Sample	Relative fluorescence signal																
	76f	100f	146f	186f	190f	209f	218f	226f	233f	242f	257f	339f	341f	351f	373f	439f	513f
LP1	0.6		0.8	1.9	0.7	0.6	0.5		0.5				2.0			1.5	93.9
LP2	12.5			1.4		3.0				3.6			13.8			8.7	59.3
LP3	5.0			1.9	1.1	2.2	1.4			1.8	1.1		15.2			2.9	70.4
LR1	54.4					2.6		0.7		18.8				1.1	2.3	3.7	17.6
LR2	58.2	1.0				4.6	0.8	1.4		5.7		0.8	1.6		0.5	3.7	23.9
LR3	65.6	1.3				12.2		2.6		1.9		2.1			2.2	3.8	14.1
PP	21.8		1.9	1.5		2.8				2.1	1.1			10.8		2.1	59.3
PR	29.7					9.9				2.7	1.5			3.4		2.1	55.9

f341 was found almost exclusively in LP samples, and f351 was most prominent in profundal samples (Table 2).

With the reverse primer, the uncut *pmoA* fragment r504 was also dominant in LP (67% ± 16%) and profundal (68% ± 2%) samples. The T-RFs r56 and r129 were present only in littoral samples, whereas the r64 fragment was present in all samples. In profundal samples, the T-RF r421 contributed to about 20% of the total fluorescence intensity and was found only in minor amounts at LR and never at LP sites (Table 3). Use of two labeled primers clearly enhanced the resolution of the T-RFLP analysis. Sequences yielding short T-RFs with one primer are especially likely to be split into different groups using the other primer. This can clearly be seen with T-RF f76, which is dominant in LR samples, but reverse T-RFs show multiple groups sharing a comparable contribution to total fluorescence intensity. Relative fluorescence intensities from the uncut PCR product varied by up to 11% (PP and PR) between both fluorescent dyes for identical samples. This variation could be explained by T-RFs that were eliminated from the analysis because of properties mentioned in the Materials and Methods section.

AMMI analysis revealed that 30.7% (0.3% noise) of the total variation among the T-RFLP profiles can be explained by the interaction of sampling location with T-RF patterns using all samples as individual environments in the analysis. The remaining variation can be attributed to differences between the replicate T-RFLP profiles. Sample heterogeneity was 1.45 in this analysis. When only littoral samples were analyzed using the three different samples from both environments (LP and LR) as replicates, 31.5% (0.3% noise) of the total variance was explained by the difference between pockmark and reference

sites. Sample heterogeneity was reduced to 1.28 by exclusion of the profundal samples.

IPCA using all samples as individual sites clearly showed that the T-RFLP profiles of samples from LP and LR sites clustered separately from each other and from the T-RFLP profiles from profundal samples, which showed no clear differences between pockmark and reference sites (Fig. 2). Another interesting finding was that LP samples cluster more closely to profundal samples than to LR samples, at least in IPCA1, which explains most of the variance. This effect could be explained mainly by the high abundance of the uncut *pmoA* fragment in both samples and disappeared if the presence of T-RFs only was analyzed (data not shown).

***pmoA* clone libraries and phylogenetic analysis.** Four separate clone libraries were generated from the *pmoA* gene fragments amplified from DNA of the littoral and profundal pockmark and reference sediment. A total of 322 clones (LP, $n = 101$; LR, $n = 72$; PP, $n = 67$; PR, $n = 82$) were analyzed and grouped according to their RFLP patterns. Of the 101 sequences obtained (LP, $n = 20$; LR, $n = 26$; PP, $n = 25$; PR, $n = 29$), 1 was identified as a chimera and was excluded from further analysis.

Clone library analysis revealed a diverse methanotrophic community of type 1 MOB. Most clones belonged to groups related to *Methylobacter* species (groups P-I to P-III, I and II, LP-I). Clones belonging to group V were also quite abundant and not closely related to any cultured MOB. Clones related to *Methylosarcina*/*Methylomicrobium* were found at all sites. No type 2 MOB or clones closely related to *Methylomonas* spp. were obtained from any sampling site. Most clones from the profundal pockmark, with only two exceptions, and all clones

TABLE 3. Relative fluorescence signals of T-RFs with fluorescence of reverse primer mb661-HEX for samples from different sampling locations

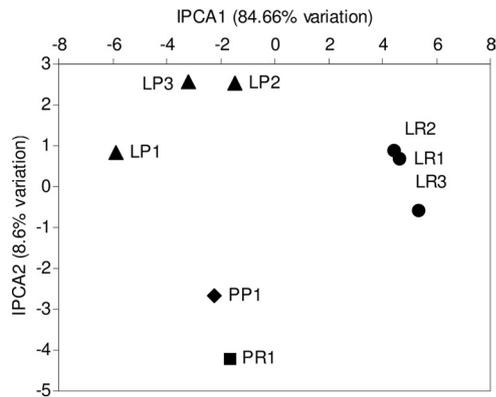| Sample	Relative fluorescence signal											
	56r	64r	69r	129r	155r	168r	257r	262r	275r	387r	421r	504r
LP1		5.7		2.3		8.5						86.0
LP2	8.6	16.8		14.6		8.6						54.8
LP3	3.6	7.1		7.0		9.0				13.5		61.2
LR1	18.3	32.2		16.6	6.2	1.9	4.5	3.2				22.3
LR2	9.1	18.4	2.7	39.5				4.5			2.0	27.2
LR3	5.3	26.5		32.5		4.3			11.0		5.5	24.2
PP		10.9			4.5						17.1	69.8
PR		9.7									27.3	66.9

FIG. 2. Plot of the interaction principal component analysis of the individual sample data sets consisting of at least 5 replicate T-RFLP profiles from each site.

from PR clearly belonged to the type 1a MOB (Fig. 3). The majority of clones obtained from littoral sediments fell into two clone groups. Most clone sequences from LP clustered in one group (LP-I) related to *Methylobacter* spp. but were distinct from all clones from other sites, and there was no closely related sequence (<93% nucleotide sequence identity; <97% amino acid sequence identity) in the NCBI database. The closest matches in the database were clones from profundal sediment of Lake Washington, near Seattle, Washington (GenBank accession number DQ067074), or a nondescribed clone from a Finnish boreal lake (GenBank accession number FN597117). On the other hand, many clones from the LR site could be assigned to type 1b MOB (group LR). This group was not detected at the other sites and belongs to a cluster that lacks any cultivated representative. The most related sequence was that of a clone from Chinese rice field soil (GenBank accession number AM910094).

When the clones were grouped using a limit of 90% sequence similarity (corresponding to 97% sequence similarity of the 16S rRNA gene [21]), the clones were grouped into 7, 12, 12, and 10 different species for LP, LR, PP, and PR, respectively. The total species richness was calculated using the chao1 estimate (26) and yielded estimated numbers of bacterial species of 12, 53, 29, and 19 for LP, LR, PP, and PR, respectively, meaning that 19 to 37% of the estimated diversity was sampled. However, these values may overestimate the overall species richness because the clones were preselected according to their restriction patterns.

Linking T-RFLP data to clone library analysis. In general, the observed T-RF sizes were shifted compared to theoretical values by from -3 bp at small T-RFs to $+2$ bp at bigger ones with FAM dye and with HEX dye by from -6 bp at small T-RFs to -8 bp at bigger ones, depending on the size of the DNA fragment. The different apparent sizes of the uncut fragment labeled with both dyes (HEX, 513 bp; FAM, 504 bp; theoretical, 508 bp) originate from internal size corrections for the different dyes, performed by the analysis software, which created wrong results if both dyes are present. The shift of the T-RFs could be verified using selected sequenced clones for T-RFLP analysis. Restriction sites corresponding to all major T-RFs were detected in the sequences used to construct the phylogenetic tree. Restriction sites corresponding to T-RFs r69, f100, f146, f186, f190, f218, f233, and f257 were not present in these data, and no reverse T-RF at 300 bp was detected, although some clones had the respective restriction site.

Assignment of T-RFs to phylogenetic groups was possible only in a few cases, because the same T-RFs were often shared by more than one phylogenetic group of MOB. However, *in silico* digestion of the clone sequences of the individual samples and the corresponding observed major T-RFLP patterns fitted well, indicating that the sequenced clones were indeed representatives of the T-RFLP patterns observed. T-RF f76 is shared by all type 1b MOB, clone PP-II434, and group P-III. Additionally, all clones of the *Methylobacter* sp. LW12-related group could clearly be assigned to T-RF r421 (429 bp). However, the reference strain *Methylocapsa acidophila* B2, a type 2 MOB, could also be assigned to this T-RF, but no phylogenetically related clone was detected. Only some clones from group LR and the related type 1b MOB *Methylococcus capsulatus* and thermophilic methanotroph HB harbor the restriction site responsible for T-RF r129 (135 bp), allowing a clear identification of this group by T-RFLP analysis. Most clones from LP have no MspI restriction site, which fits very well to the T-RFLP patterns (Tables 2 and 3).
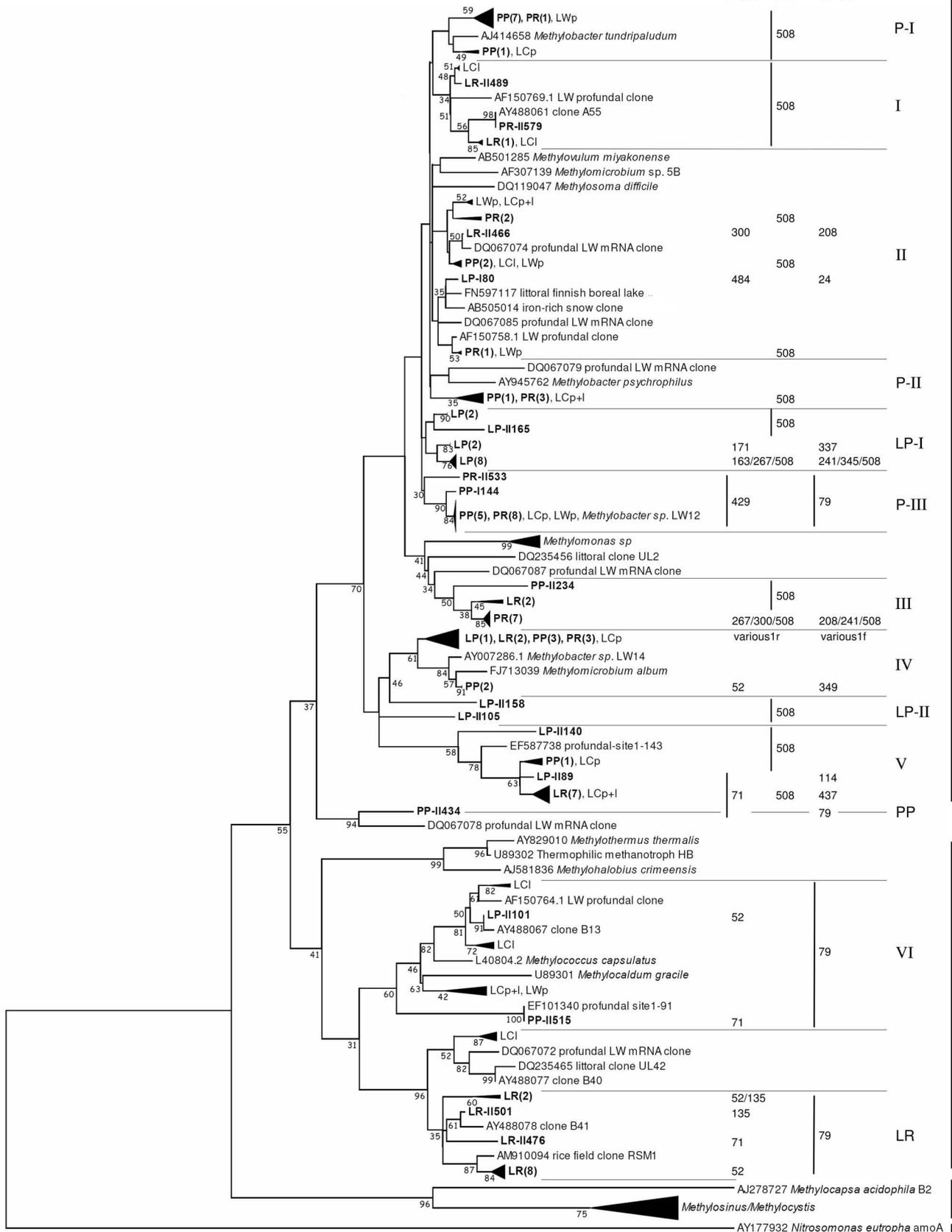
Quantitative real-time PCR. Quantitative real-time PCR was used to estimate the abundance of methanotrophic bacteria at the different locations. This technique yielded no unspecific PCR products, thus allowing a quantification of the *pmoA* gene in all samples. In the littoral pockmark samples PM1 and PM3, MOB abundances were significantly higher than in the other samples ($2.5 \times 10^9 \pm 1.6 \times 10^9$ and $1.1 \times 10^9 \pm 0.7 \times 10^9$ cells per gram sediment wet weight, respectively). In profundal samples, MOB numbers were 1 order of magnitude lower, with $1.0 \times 10^8 \pm 0.3 \times 10^8$ and $7.3 \times 10^8 \pm 2.1 \times 10^7$ cells per gram in PP and PR, respectively. Littoral reference samples and LP2 had the lowest abundances of methanotrophic bacteria, in the range from 3.2×10^6 (LR3) to 3.7×10^7 (LR1) cells per gram sediment (wet weight) (Table 1). Melting curve analysis showed slightly variable melting temperatures of the PCR products between 82°C and 85°C for all samples, but all LR samples showed another maximum at 88 to 90°C (data not shown).

DISCUSSION

Methane oxidation capacities. Methane oxidation capacities or potential methane oxidation rates were determined to estimate the methanotrophic potential present in the respective sediments. Although they do not directly reflect methane oxidation rates *in situ*, they can serve as a measure for the abundance and activity of the methanotrophic communities present.

Methane oxidation capacities at pockmarks were found to be substantially higher than those in the surrounding sediment, indicating that they can be considered hot spots of methanotrophic activity in an otherwise oligotrophic environment. These differences are likely to be even higher at a higher spatial resolution, since the slurry for the experiments in this study was prepared from a total of 113 to 200 ml sediment, thus diluting the high methanotrophic activity that might be concentrated in a few ml at close proximity to the gas emanation site. Such spatial heterogeneity may also explain why the meth-

| | Terminal Restriction Sites | | | Group |
	reverse	both	forward	

_59_ **PP(7), PR(1)**, LWp
AJ414658 _Methylobacter tundripaludum_ — 508 — P-I
_49_ **PP(1)**, LCp

_51_ LCl
_48_ **LR-II489**
_34_ AF150769.1 LW profundal clone — 508 — I
_51_ _98_ AY488061 clone A55
_56_ **PR-II579**
_85_ **LR(1)**, LCl

AB501285 _Methylovulum miyakonense_
AF307139 _Methylomicrobium sp._ 5B
DQ119047 _Methylosoma difficile_
_52_ LWp, LCp+l
PR(2) — — 508
_50_ **LR-II466** — 300 — 208
DQ067074 profundal LW mRNA clone
PP(2), LCl, LWp — — 508 — II
LP-I80 — 484 — 24
_35_ FN597117 littoral finnish boreal lake
AB505014 iron-rich snow clone
DQ067085 profundal LW mRNA clone
AF150758.1 LW profundal clone
_53_ **PR(1)**, LWp — — 508

DQ067079 profundal LW mRNA clone
AY945762 _Methylobacter psychrophilus_ — P-II
_35_ **PP(1), PR(3)**, LCp+l — — 508
_90_ **LP(2)**
_83_ **LP-II165** — — 508 — LP-I
_76_ **LP(2)** — 171 — 337
LP(8) — 163/267/508 — 241/345/508

PR-II533
_30_ **PP-I144** — — — P-III
_90_ **PP(5), PR(8)**, LCp, LWp, _Methylobacter sp._ LW12 — 429 — 79
_84_

_99_ _Methylomonas sp_
DQ235456 littoral clone UL2
_41_ DQ067087 profundal LW mRNA clone
_44_ **PP-II234** — — 508 — III
_34_ _45_ **LR(2)**
_50_ _38_ **PR(7)** — 267/300/508 — 208/241/508
_85_

LP(1), LR(2), PP(3), PR(3), LCp — various1r — various1f
_61_ AY007286.1 _Methylobacter sp._ LW14
_84_ FJ713039 _Methylomicrobium album_ — IV
_46_ _57_ **PP(2)** — 52 — 349
_91_

LP-II158
LP-II105 — — 508 — LP-II
_37_

LP-II140
EF587738 profundal-site1-143 — — 508 — V
_58_ **PP(1)**, LCp
_78_ **LP-II89** — — — 114
_63_ **LR(7)**, LCp+l — 71 — 508 — 437

PP-II434 — — — 79 — PP
_55_ _94_ DQ067078 profundal LW mRNA clone

_70_ AY829010 _Methylothermus thermalis_
_96_ U89302 Thermophilic methanotroph HB
_99_ AJ581836 _Methylohalobius crimeensis_

_82_ LCl
_61_ AF150764.1 LW profundal clone
_50_ **LP-II101** — 52
_91_ AY488067 clone B13
_81_ LCl — 79 — VI
_82_ _72_
L40804.2 _Methylococcus capsulatus_
_46_ U89301 _Methylocaldum gracile_
_60_ _63_ _42_ LCp+l, LWp
EF101340 profundal site1-91
_100_ **PP-II515** — 71

_41_ _87_ LCl
_52_ DQ067072 profundal LW mRNA clone
_82_ DQ235465 littoral clone UL42
_99_ AY488077 clone B40

_31_ **LR(2)** — 52/135
_60_ **LR-II501** — 135
_96_ _61_ AY488078 clone B41 — — — 79 — LR
_35_ **LR-II476** — 71
AM910094 rice field clone RSM1
_87_ **LR(8)** — 52
_84_

AJ278727 _Methylocapsa acidophila_ B2
_96_ _75_ _Methylosinus/Methylocystis_
AY177932 _Nitrosomonas eutropha_ amoA

Type 1a
Type 1b
Type 2

0.05

ane oxidation capacities of core LP2 were lower by 1 order of magnitude than those of the other LP samples, even though all littoral samples were taken by trained scientific divers right at the respective gas emanation sites. Our data confirm earlier results derived from methane concentration profiles which indicated that *in situ* methane oxidation rates at pockmarks were 20 times higher than those in the surrounding sediment (6). The comparably small but still substantial differences between methane oxidation activities at the PP site versus the PR site can also be explained by sampling inaccuracies, even though a horizontal sonar was employed to direct the multicorer into the center of the profundal pockmarks. These results are consistent with the low geochemical differences observed for these sites (6).

The methane oxidation capacities measured inside LPs were comparable to those measured previously in sediment slurries taken in summertime from the Obere Güll, a shallow bay in Lake Constance (4), where maximal methane oxidation capacities of about 1 $\mu mol\ ml_{sed}^{-1}\ h^{-1}$ (where the subscript sed indicates sediment) and half-saturation constants of 3.5 to 11 μM were measured. These sediments are oversaturated with methane in summertime, since both methane production and methane oxidation are seasonally fluctuating processes even in the profundal zone of temperate lakes, with 5- to 20-fold changes reported in Lake Constance (44, 49).

Sediments of Lake Washington, a comparable, well-investigated oligotrophic freshwater lake, showed maximal oxidation rates of 7.2 to 41.3 $nmol\ ml_{sed}^{-1}\ h^{-1}$ at the sediment-water interface and 0.27 to 4.5 $nmol\ ml_{sed}^{-1}\ h^{-1}$ in deeper layers (65 m water depth) of profundal sediment (31). Those values are similar to those obtained in our study for reference sediments outside the pockmarks (Table 1). However, $S_{0.5}$ values were slightly higher in Lake Washington (9.5 ± 1.2 μM) than in the reference sediment in our study (2 to 5 μM). Another study (2) found significantly higher rates of 364 $nmol\ ml_{sed}^{-1}\ h^{-1}$ in the uppermost 0.5 cm of profundal Lake Washington sediment and slightly lower rates below that zone, reaching methane oxidation capacities comparable to the rates found at littoral pockmark sites.

Qualitative analysis of methane-oxidizing communities. Molecular community analysis revealed a picture that corresponds well with the measurements of the methane oxidation capacities. T-RFLP analysis showed considerable differences between pockmark and reference sediments in the littoral zone and less pronounced differences between the profundal sediments. These patterns accounted for 30% variance in the AMMI analysis of the T-RFLP data, which is comparable to that for other environmental samples (11, 12). Interestingly, the community composition in LP2, which showed clear differences in methane oxidation capacities, was very similar to that in the other LP samples, confirming that samples were taken in close proximity to the gas emanation site. Unfortunately, we were not able to relate all T-RFs to defined phylogenetic groups with our data set, like other studies (30, 32, 45), because the same T-RFs were often shared by more than one phylogenetic group of MOB or pseudo-T-RFs rendered a clear phylogenetic assignment barely possible (15). However, differences in community structure of MOB between LP, LR, and profundal sites were clearly reproduced.

Clone library analysis verified the differences between MOB communities at the different sites and revealed the identities of the MOB groups that form these differences. In the littoral zone, type 1b MOB were abundant at the reference site, whereas group LP-I appears to dominate the MOB community and to benefit from the conditions at the pockmark site. *In silico* digestion of the clones mirrors the major features of the obtained T-RFLP profiles, suggesting that the abundant MOB groups were covered in our analysis. A PCR bias toward type 1 MOB has been reported for primer mb661 and might explain the lack of type II MOB-affiliated sequences in our analyses, even though primer mb661 also amplified type II MOB from environmental samples (5). The results of phylogenetic analysis of clone libraries obtained in this study were mostly congruent with those of previous studies performed for Lake Constance and Lake Washington (2, 10, 35, 40). *Methylobacter*-like MOB appeared to be dominant, especially in the profundal part of the lake. In contrast to previous studies (40), type 1b MOB constituted a significant part of the MOB community in littoral reference sediment, in particular, group LR, which is related to sequences often found in rice field soils (38). However, a study using the A189-A682 primer pair (23) found type II and type 1b MOB in littoral sediments obtained from Obere Güll (35). These variances in the community structure between different studies on Lake Constance can be explained by temporal variations or environmental conditions between different parts of the lake, e.g., input of allochthonous carbon and nutrients by the Rhine River (46) or exposure to mechanical disturbance (22). This might also be a reason for the observed similarities between LP and profundal sites, as the pockmark structure might provide some shelter against disturbing environmental factors. However, despite known correlations between MOB occurrence and environmental factors (19, 20, 30, 33) or the results of direct competition experiments (1, 18, 20, 47), the physiological reasons for the observed distribution of different MOB strains in their environmental niches are still largely unknown.

Quantitative analysis of methane-oxidizing communities. The abundance of methanotrophic bacteria at the different sites correlated well with the observed methane oxidation capacities, suggesting that high methane oxidation capacities were caused by high MOB abundances. Absolute MOB cell numbers obtained in previous studies from Lake Constance

FIG. 3. Phylogenetic dendrogram of deduced PmoA sequences (169 amino acids). The tree was constructed using the minimum-evolution method in MEGA (version 4) software, selecting the pairwise deletion option. Bootstrap values (1,000 replicates) are shown next to the branches. The evolutionary distances were calculated using the JTT matrix-based method. Clones obtained in this study are shown in boldface, and numbers in parentheses represent the numbers of clones in a collapsed subtree. Theoretical T-RF sizes are given for reverse and forward primers or, in case of the uncut PCR product, for T-RFs shared by both primers. Groups are labeled as mentioned in the text. LW, Lake Washington; LC, Lake Constance; p, profundal; l, littoral; various1r, 71, 159, 267, and 508 bp; various1f, 33, 158, 241, 437, and 508 bp.

and Lake Washington agree with those from our reference sediments (9, 39). When MOB cell numbers were calculated on the basis of the methane oxidation capacities of the sediments using a maximum methane oxidation activity per cell of 0.5×10^{-6} to 3×10^{-6} nmol h^{-1} (9), cell numbers were, on average, more than 1 order of magnitude lower than cell numbers obtained by qPCR. This indicates that major parts of the MOB communities present in the sediments were inactive or resting. Similar results were obtained previously when MOB cell counts obtained by fluorescence *in situ* hybridization and qPCR were compared (39). Absolute copy numbers or cell numbers have to be treated with caution, because the use of external standards is error prone and the heterogeneity between environmental samples like sediments can cause variations in DNA extraction and PCR efficiencies. However, in this study MOB abundances differed by orders of magnitude between different samples, thus clearly identifying pockmarks as hot spots of methane oxidation and MOB abundance.

Melting curve analysis after qPCR showed slight differences between samples reflecting different *pmoA* sequences, and in LR samples an additional distinct peak occurred at increased temperatures that can be attributed to the higher GC content of the *pmoA* fragments obtained from type 1b MOB. Therefore, melting curve analysis and especially high-resolution melting curve analysis could serve as tools to access quickly the diversity of, e.g., *pmoA* genes also in environmental samples. In our study, it verified the differences in community composition obtained by clone library analysis.

Collectively, potential methane oxidation rates as well as various molecular methods identified pockmarks as hot spots of methanotrophic activity and abundance and as environmental niches in Lake Constance that are occupied by distinct strains of MOB, especially in the littoral zone. Furthermore, the results show once again that entire groups of MOB detected by molecular methods lack cultivated representatives and, thus, lack physiological information that might be crucial to understand the distribution and ecology of MOB in their natural environments.

REFERENCES

1. **Amaral, J. A., and R. Knowles.** 1995. Growth of methanotrophs in methane and oxygen counter gradients. FEMS Microbiol. Lett. **126:**215–220.
2. **Auman, A. J., S. Stolyar, A. M. Costello, and M. E. Lidstrom.** 2000. Molecular characterization of methanotrophic isolates from freshwater lake sediment. Appl. Environ. Microbiol. **66:**5259–5266.
3. **Bastviken, D., J. Cole, M. Pace, and L. Tranvik.** 2004. Methane emissions from lakes: dependence of lake characteristics, two regional assessments, and a global estimate. Global Biogeochem. Cy. **18.** doi:10.1029.2004GB002238.
4. **Bosse, U., P. Frenzel, and R. Conrad.** 1993. Inhibition of methane oxidation by ammonium in the surface layer of a littoral sediment. FEMS Microbiol. Ecol. **13:**123–134.
5. **Bourne, D. G., I. R. McDonald, and J. C. Murrell.** 2001. Comparison of *pmoA* PCR primer sets as tools for investigating methanotroph diversity in three Danish soils. Appl. Environ. Microbiol. **67:**3802–3809.
6. **Bussmann, I., S. Schloemer, M. Schlüter, and M. Wessels.** 2011. Active pockmarks in a large lake (Lake Constance, Germany): effects on methane distribution and turnover in the sediment. Limnol. Oceanogr. **56:**379–393.
7. **Bussmann, I., M. Pester, A. Brune, and B. Schink.** 2004. Preferential cultivation of type II methanotrophic bacteria from littoral sediments (Lake Constance). FEMS Microbiol. Ecol. **47:**179–189.
8. **Conrad, R.** 2009. The global methane cycle: recent advances in understanding the microbial processes involved. Environ. Microbiol. Rep. **1:**285–292.
9. **Costello, A. M., A. J. Auman, J. L. Macalady, K. M. Scow, and M. E. Lidstrom.** 2002. Estimation of methanotroph abundance in a freshwater lake sediment. Environ. Microbiol. **4:**443–450.
10. **Costello, A. M., and M. E. Lidstrom.** 1999. Molecular characterization of functional and phylogenetic genes from natural populations of methanotrophs in lake sediments. Appl. Environ. Microbiol. **65:**5066–5074.
11. **Culman, S. W., R. Bukowski, H. G. Gauch, H. Cadillo-Quiroz, and D. H. Buckley.** 2009. T-REX: software for the processing and analysis of T-RFLP data. BMC Bioinformatics **10:**171.
12. **Culman, S. W., H. G. Gauch, C. B. Blackwood, and J. E. Thies.** 2008. Analysis of T-RFLP data using analysis of variance and ordination methods: a comparative study. J. Microbiol. Methods **75:**55–63.
13. **DelSontro, T., D. F. McGinnis, S. Sobek, I. Ostrovsky, and B. Wehrli.** 2010. Extreme methane emissions from a Swiss hydropower reservoir: contribution from bubbling sediments. Environ. Sci. Technol. **44:**2419–2425.
14. **Duck, R. W., and R. A. Herbert.** 2006. High-resolution shallow seismic identification of gas escape features in the sediments of Loch Tay, Scotland: tectonic and microbiological associations. Sedimentology **53:**481–493.
15. **Egert, M., and M. W. Friedrich.** 2003. Formation of pseudo-terminal restriction fragments, a PCR-related bias affecting terminal restriction fragment length polymorphism analysis of microbial community structure. Appl. Environ. Microbiol. **69:**2555–2562.
16. **Etiope, G.** 2004. New directions: GEM—geologic emissions of methane, the missing source in the atmospheric methane budget. Atmos. Environ. **38:** 3099–3100.
17. **Frenzel, P., B. Thebrath, and R. Conrad.** 1990. Oxidation of methane in the oxic surface-layer of a deep lake sediment (Lake Constance). FEMS Microbiol. Ecol. **73:**149–158.
18. **Graham, D. W., J. A. Chaudhary, R. S. Hanson, and R. G. Arnold.** 1993. Factors affecting competition between type-I and type-II methanotrophs in 2-organism, continuous-flow reactors. Microb. Ecol. **25:**1–17.
19. **Henckel, T., U. Jackel, and R. Conrad.** 2001. Vertical distribution of the methanotrophic community after drainage of rice field soil. FEMS Microbiol. Ecol. **34:**279–291.
20. **Henckel, T., P. Roslev, and R. Conrad.** 2000. Effects of O_2 and CH_4 on presence and activity of the indigenous methanotrophic community in rice field soil. Environ. Microbiol. **2:**666–679.
21. **Heyer, J., V. F. Galchenko, and P. F. Dunfield.** 2002. Molecular phylogeny of type II methane-oxidizing bacteria isolated from various environments. Microbiology **148:**2831–2846.
22. **Hofmann, H., A. Lorke, and F. Peeters.** 2008. Temporal scales of water-level fluctuations in lakes and their ecological implications. Hydrobiologia **613:** 85–96.
23. **Holmes, A. J., A. Costello, M. E. Lidstrom, and J. C. Murrell.** 1995. Evidence that particulate methane monooxygenase and ammonia monooxygenase may be evolutionarily related. FEMS Microbiol. Lett. **132:**203–208.
24. **Hovland, M., J. V. Gardner, and A. G. Judd.** 2002. The significance of pockmarks to understanding fluid flow processes and geohazards. Geofluids **2:**127–136.
25. **Hovland, M., and A. G. Judd.** 1988. Seabed pockmarks and seepages. Impact on geology, biology and the marine environment. Graham & Trotman Ltd., London, United Kingdom.
26. **Hughes, J. B., J. J. Hellmann, T. H. Ricketts, and B. J. M. Bohannan.** 2001. Counting the uncountable: statistical approaches to estimating microbial diversity. Appl. Environ. Microbiol. **67:**4399–4406.
27. **IPCC.** 2007. Climate change 2007: the physical science basis. *In* S. Solomon et al. (ed.), contribution of Working Group I to the Fourth Assessment Report of the Intergovernmental Panel on Climate Change. Cambridge University Press, Cambridge, United Kingdom.
28. **Judd, A., and M. Hovland.** 2007. Seabed fluid flow. Cambridge University Press, Cambridge, United Kingdom.
29. **Kolb, S., C. Knief, S. Stubner, and R. Conrad.** 2003. Quantitative detection of methanotrophs in soil by novel *pmoA*-targeted real-time PCR assays. Appl. Environ. Microbiol. **69:**2423–2429.
30. **Krause, S., C. Luke, and P. Frenzel.** 2010. Succession of methanotrophs in oxygen-methane counter-gradients of flooded rice paddies. ISME J. **4:**1603–1607.
31. **Lidstrom, M. E., and L. Somers.** 1984. Seasonal study of methane oxidation in Lake Washington. Appl. Environ. Microbiol. **47:**1255–1260.
32. **Luke, C., et al.** 2010. Biogeography of wetland rice methanotrophs. Environ. Microbiol. **12:**862–872.
33. **Macalady, J. L., A. M. S. McMillan, A. F. Dickens, S. C. Tyler, and K. M. Scow.** 2002. Population dynamics of type I and II methanotrophic bacteria in rice soils. Environ. Microbiol. **4:**148–157.

34. **Noll, M., D. Matthies, P. Frenzel, M. Derakshani, and W. Liesack.** 2005. Succession of bacterial community structure and diversity in a paddy soil oxygen gradient. Environ. Microbiol. **7:**382–395.

35. **Pester, M., M. W. Friedrich, B. Schink, and A. Brune.** 2004. *pmoA*-based analysis of methanotrophs in a littoral lake sediment reveals a diverse and stable community in a dynamic environment. Appl. Environ. Microbiol. **70:**3138–3142.

36. **Pickrill, R. A.** 1993. Shallow seismic stratigraphy and pockmarks of a hydrothermally influenced lake, Lake Rotoiti, New Zealand. Sedimentology **40:**813–828.

37. **Platen, H., and B. Schink.** 1987. Methanogenic degradation of acetone by an enrichment culture. Arch. Microbiol. **149:**136–141.

38. **Qiu, Q., M. Noll, W.-R. Abraham, Y. Lu, and R. Conrad.** 2008. Applying stable isotope probing of phospholipid fatty acids and rRNA in a Chinese rice field to study activity and composition of the methanotrophic bacterial communities in situ. ISME J. **2:**602–614.

39. **Rahalkar, M., J. Deutzmann, B. Schink, and I. Bussmann.** 2009. Abundance and activity of methanotrophic bacteria in littoral and profundal sediments of Lake Constance (Germany). Appl. Environ. Microbiol. **75:**119–126.

40. **Rahalkar, M., and B. Schink.** 2007. Comparison of aerobic methanotrophic communities in littoral and profundal sediments of Lake Constance by a molecular approach. Appl. Environ. Microbiol. **73:**4389–4394.

41. **Reay, D.** 2010. Methane and climate change. Earthscan, London, United Kingdom.

42. **Rudd, J. W. M., and C. D. Taylor.** 1980. Methane cycling in aquatic environments. Adv. Aquat. Microbiol. **2:**77–150.

43. **Ruijter, J. M., et al.** 2009. Amplification efficiency: linking baseline and bias in the analysis of quantitative PCR data. Nucleic Acids Res. **37:**e45.

44. **Schulz, S., and R. Conrad.** 1995. Effect of algal deposition on acetate and methane concentrations in the profundal sediment of a deep lake (Lake Constance). FEMS Microbiol. Ecol. **16:**251–259.

45. **Shrestha, M., W.-R. S. P. M. Abraham, M. Noll, and R. Conrad.** 2008. Activity and composition of methanotrophic bacterial communities in planted rice soil studied by flux measurements, analyses of *pmoA* gene and stable isotope probing of phospholipid fatty acids. Environ. Microbiol. **10:**400–412.

46. **Sobek, S., et al.** 2009. Organic carbon burial efficiency in lake sediments controlled by oxygen exposure time and sediment source. Limnol. Oceanogr. **54:**2243–2254.

47. **Steenbergh, A. K., M. M. Meima, M. Kamst, and P. L. E. Bodelier.** 2010. Biphasic kinetics of a methanotrophic community is a combination of growth and increased activity per cell. FEMS Microbiol. Ecol. **71:**12–22.

48. **Tamura, K., J. Dudley, M. Nei, and S. Kumar.** 2007. MEGA4: molecular evolutionary genetics analysis (MEGA) software version 4.0. Mol. Biol. Evol. **24:**1596–1599.

49. **Thebrath, B., F. Rothfuss, M. J. Whiticar, and R. Conrad.** 1993. Methane production in littoral sediment of Lake Constance. FEMS Microbiol. Ecol. **102:**279–289.

50. **Wessels, M., I. Bussmann, S. Schloemer, M. Schlüter, and V. Böder.** 2010. Distribution, morphology, and formation of pockmarks in Lake Constance. Limnol. Oceanogr. **55:**2623–2633.